Anal. Chem. **2002,** *74,* 232−238

Single-Particle Mass Spectrometry of Polystyrene Microspheres and Diamond Nanocrystals

Y. Cai,[†] W.-P. Peng,[†] S.-J. Kuo,[‡] Y. T. Lee,[†,‡] and H.-C. Chang*[,†]

Institute of Atomic and Molecular Sciences, Academia Sinica, P.O. Box 23-166, Taipei, Taiwan 106, and Department of Chemistry, National Taiwan University, Taipei, Taiwan 106

High-resolution mass spectra of single submicrometer-sized particles are obtained using an electrospray ionization source in combination with an audio frequency quadrupole ion-trap mass spectrometer. Distinct from conventional methods, light scattering from a continuous Ar-ion laser is detected for particles ejected out of the ion trap. Typically, 10 particles are being trapped and interrogated in each measurement. With the audio frequency ion trap operated in a mass-selective instability mode, analysis of the particles reveals that they all differ in mass-to-charge ratio (m/z), and the individual peak in the observed mass spectrum is essentially derived from one single particle. A histogram of the spectra acquired in 10^2 repetitions of the experiment is equivalent to the single spectrum that would be observed when an ion ensemble of 10^3 particles is analyzed simultaneously using the single-particle mass spectrometer (SPMS). To calibrate such single-particle mass spectra, secular frequencies of the oscillatory motions of the individual particle within the trap are measured, and the trap parameter q_z at the point of ejection is determined. A mass resolution exceeding 10^4 can readily be achieved in the absence of ion ensemble effect. We demonstrate in this work that the SPMS not only allows investigations of monodisperse polystyrene microspheres, but also is capable of detecting diamond nanoparticles with a nominal diameter of 100 nm, as well.

Electrospray ionization (ESI), first introduced to the scientific community in 1984,[1] has been demonstrated to be such a versatile tool that it can bring a wide range of intact macroions from solution into the gas phase for mass spectral analysis. Macroions of both biological and synthetic polymers are amendable to close examination in a solvent-free environment.[2] Moreover, single ions can be interrogated individually. This has been realized by Smith and co-workers[3,4] for multiply charged particles using a Fourier transform ion cyclotron resonance (FTICR) mass spectrometer. Although detection of single ions by ESI−FTICR may probably provide the highest accuracy in both charge state and molecular weight determination of macroions, the spectrometer is not quite suitable for rapid and routine analysis of bulk samples. Benner and co-workers[5,6] have developed a simplified version of the technique, which similarly measures the ion image current of multiply charged macromolecules using a nondestructive, charge-sensitive detector. Applications of the technique to mass/charge analysis of submicrometer-sized polystyrene particles (with a mean mass of 1×10^{10} Da) have also been attempted;[5] however, accuracy of the measurements is largely limited by the lack of a good control of particle velocity as a result of gas flowing through the ESI source.

Despite that much progress in the field of mass spectrometry has been made for macroions, there remains a challenge to acquire high-resolution mass spectra of particles having a mass-to-charge ratio (m/z) higher than 10^6. A technique that has been developed to analyze microparticles is known as the aerosol beam spectrometry.[7] It is a special kind of time-of-flight mass spectrometry that takes advantage of aerodynamics, instead of electrostatics, to separate particles of different sizes. The method demonstrates a utility of separating particles having a difference of 10% in aerodynamic size, but determination of the charge states of ionized particles is not feasible using this aerosol beam spectrometer. Electrophoretic mobility of singly charged ions in ambient air has also been utilized to separate nanometer-sized particles of biological interest.[8] The technique involves the use of a cloud chamber filled with saturating butanol vapor as a detector for these bioparticles, which otherwise cannot be probed directly using elastic light-scattering methods.

Quadrupole ion trap (QIT) is a device that can confine a wide variety of charged species into a space for detailed examination.[9] The capability of trapping and detection of single microparticles

* E-mail: hcchang@po.iams.sinica.edu.tw.
[†] Institute of Atomic and Molecular Sciences.
[‡] Department of Chemistry, National Taiwan University.

(1) Yamashita, M.; Fenn, J. B. *J. Phys. Chem.* **1984**, *88*, 4451−4459. Fenn, J. B.; Mann, M.; Meng, C. K.; Wong, S. F.; Whitehouse, C. M. *Science* **1989**, *246*, 64−71.
(2) Nohmi, T.; Fenn, J. B. *J. Am. Chem. Soc.* **1992**, *114*, 3241−3246.
(3) Smith, R. D.; Cheng, X.; Bruce, J. E.; Hofstadler, S. A.; Anderson, G. A. *Nature* **1994**, *369*, 137−139. Bruce, J. E.; Cheng, X.; Bakhtiar, R.; Wu, Q.; Hofstadler, S. A.; Anderson, G. A.; Smith, R. D. *J. Am. Chem. Soc.* **1994**, *116*, 7839−7847.
(4) Cheng, X.; Bakhtiar, R.; Van Orden, S.; Smith, R. D. *Anal. Chem.* **1994**, *66*, 2084−2087.
(5) Fuerstenau, S. D.; Benner, W. H. *Rapid Commun. Mass Spectrom.* **1995**, *9*, 1528−1538.
(6) Fuerstenau, S. D.; Benner, W. H.; Thomas, J. J.; Brugidou, C.; Bothner, B.; Siuzdak, G. *Angew. Chem., Int. Ed.* **2001**, *40*, 541−544.
(7) Dahneke, B. *Nat. Phys. Sci.* **1973**, *244*, 54−55.
(8) Kaufman, S. L.; Skogen, J. W.; Dorman, F. D.; Zarrin, F.; Lewis, K. C. *Anal. Chem.* **1996**, *68*, 1895−1904.
(9) March, R. E.; Hughes, R. J. *Quadrupole Storage Mass Spectrometer*; Wiley: New York, 1989.

10.1021/ac010776y CCC: $22.00
Published on Web 11/28/2001

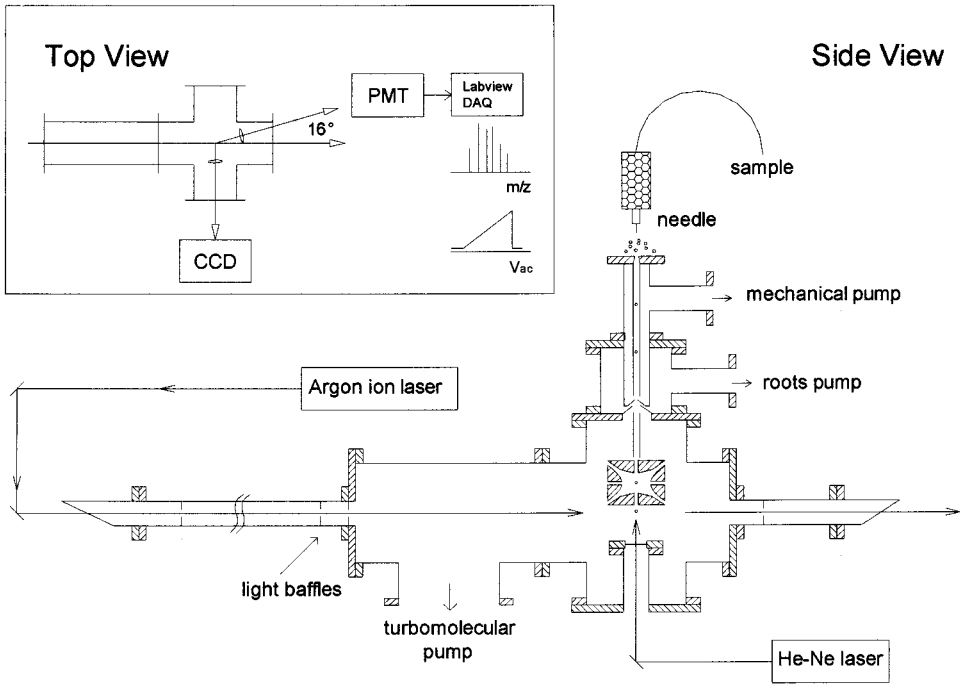

Figure 1. Schematic diagrams of the experimental setup. Note that the CCD camera and the PMT detector are located at two different levels that are separated by about 20 mm.

in such a device was first illustrated by Wuerker et al. in 1959.[10] Many attempts[11−16] followed and aimed at determining the absolute mass of a single levitated particle using either charge differential[13] or star branch counting[15] methods. A mass resolution ($m/\Delta m$) on the order of 10^3 or better for particles weighing 10^{-16} kg can readily be attained. Gerlich and co-workers[17] recently addressed an interesting possibility of utilizing this three-dimensional ion trap as a nanoparticle mass spectrometer. High-precision measurements with an uncertainty of 10^{-4} in mass determination and ± 1 in charge state determination were accomplished. Analogous to the single-ion detection of Smith et al.,[3] however, the data taken from such a nanoparticle mass spectrometer are not in the form of a true mass spectrum, because the particles are analyzed only one at a time.

We report herein the result of our attempt to construct a single-particle mass spectrometer (SPMS)[18] for rapid and routine analysis of the mass and charge state of nanometer-sized particles. The attempt involves a combination of methods, such as ESI, QIT, and scattered light detection. The SPMS has three important characteristics. First, the ion trap is driven by an audio frequency (AF) power amplifier optimized at 50−2000 Hz, rather than at 1 MHz, as used by conventional ESI−QIT mass spectrometers.[19,20] Second, collecting scattered light from a continuous Ar-ion laser is utilized as a method for particle detection. Third, the individual peaks in the observed spectrum are derived from single particles instead of ion ensembles, thereby allowing high-resolution mass spectrometric measurements to be performed for submicrometer-sized or nanometer-sized particles.

EXPERIMENTAL SECTION

The Setup. Figure 1 depicts a schematic diagram of the experimental setup, which consists of three interoperative parts:

(1) Electrospray Ionization Source. The ESI source shown in Figure 1 comprises a needle (200 μm i.d.) and a flat entrance plate with an orifice diameter of 150 μm. A 4 kV dc is applied to the needle with respect to the plate, which is kept at ground potential during the operation. The ESI-generated particles, after passing through the orifice, are guided by a beam tube (4-mm i.d. and 150-mm length) to the first skimmer (orifice diameter, 700 μm), which separates the first from the second differentially pumped chamber. The pressure inside these two chambers is maintained at 1 Torr by a 12 L/s mechanical pump and at 1 mTorr by a 50 L/s Roots pump, respectively. Carried by the gas flow, the particles pass through the second skimmer (1.5-mm orifice diameter) and enter the ion trap chamber, evacuated by a 250 L/s turbomolecular pump to a pressure of 7×10^{-5} Torr. The second beam tube directs the particles toward the entrance hole of the ion trap for electrodynamic confinement. Once the particles of interest are confined, the ESI source is turned off, the hole on the entrance plate is sealed, and a base pressure of

(10) Wuerker, R. F.; Shelton, H.; Langmuir, R. V. *J. Appl. Phys.* **1959**, *30*, 342−349.
(11) A review on the detection and analysis of a single trapped particle has been given by Davis, E. J. *Aerosol Sci. Technol.* **1997**, *26*, 212−254.
(12) Davis, E. J.; Ray, A. K. *J. Colloid Interface Sci.* **1980**, *75*, 566−576.
(13) Philip, M. A.; Gelbard, F.; Arnold, S. *J. Colloid Interface Sci.* **1983**, *91*, 507−515.
(14) Winter, H.; Ortjohann, H. W. *Am. J. Phys.* **1991**, *59*, 807−813.
(15) Hars, G.; Tass, Z. *J. Appl. Phys.* **1995**, *77*, 4245−4250.
(16) Schlemmer, S.; Illemann, J.; Wellert, S.; Gerlich, D. *J. Appl. Phys.*, submitted.
(17) Gerlich, D.; Illemann, J.; Schlemmer, S. In *Molecular Hydrogen in Space*; Combes, F., Pineau des Forets, G., Eds.; Cambridge University Press: Stanford, 2000.
(18) Relevant studies on the mass spectrometric analysis of single aerosols can be found in Noble, C. A.; Prather, K. A. *Mass Spectrom. Rev.* **2000**, *19*, 248−274.
(19) Van Berkel, G. J.; Glish, G. L.; McLuckey, S. A. *Anal. Chem.* **1990**, *62*, 1284−1295.
(20) Kaiser, R. E., Jr.; Cooks, R. G.; Stafford, G. C., Jr.; Syka, J. E. P.; Hemberger, P. H. *Int. J. Mass Spectrom. Ion Processes* **1991**, *106*, 79−115.

2×10^{-6} Torr is reached. The typical trapping time of the particles prior to ejection is 30 s.

No capillary is adopted in this apparatus, because it has been empirically found that with use of the capillary, the particles would become less positively charged as a result of multiple charge uptake from the walls via collisions.[21] All of the beam tubes and skimmers shown in Figure 1 are therefore grounded, as the movement of the submicrometer-sized particles within the apparatus is dominated by aerodynamics, rather than by electrostatics. A vertical beam axis is further chosen to avoid loss of the particles due to gravitational settling.

(2) Quadrupole Ion Trap. The QIT device, manufactured by Jordan, has a size parameter of $z_0 = 7.07$ mm and other characteristics essentially identical to that of the ion trap detector.[20] It was modified in such a way that six holes (3.1-mm diameter) lying on three perpendicular axes are drilled on the ring electrode and end caps. Applied to the two end caps is a frequency-variable ac voltage from a high-voltage transformer driven by an AF power amplifier and a synthesized function generator. The ring electrode is grounded, and so the two end caps can be floated at a small dc voltage to balance the gravitational force.[10]

To acquire mass spectra, a standard mass-selective instability mode is used to select the ions of interest by scanning the end-cap voltage to empty the trap. Before the voltage scans, the chamber is back-filled with He buffer gas to 1 mTorr to retain the particles in the trap center and, at the same time, to reduce both the radial and axial amplitudes of their oscillatory motions. The ac voltage amplitude (V_{ac}) is varied from 420 to 1700 V during the course of the particle ejection to obtain a full scan of the spectrum.

(3) Scattered Light Detection System. A polarized Ar ion laser is employed as the illuminator for particles ejected out of the ion trap through the hole on the lower end cap. To ensure that all of the particles are detected, the laser beam ($\lambda = 514.5$ nm) is self-expanded to a diameter of 3 mm without use of a beam expander. The typical power density at the point of light scattering is 10 kW/m^2. As depicted in Figure 1, the laser enters the chamber through a Brewster angle window situated about 1.3 m away from the scatterers. Three apertures with orifices of 8, 10, and 12 mm in diameter are positioned along the way, behaving like light baffles, to minimize background signals arising from scattering and reflection of the laser beam from either the window or the wall of the chamber. A photomultiplier tube (PMT) serves to collect the light pulses produced by the particles traversing through the laser beam at a forward scattering angle of 16°.[22]

Amino-Polystyrene Particles. The sample consists of a colloidal suspension (Spherotech AP-08-10) containing 5.0% (w/v) monodisperse amino-polystyrene particles with a mean diameter of $2a = 0.91 \pm 0.022$ μm. To minimize surface cationization during ESI, the particles are thoroughly washed with deionized water and acidified with acetic acid before use. One unique feature of these particles is that their surfaces are functionalized with the aminoheptyl group [$-(CH_2)_7NH_2$] at a concentration of 3×10^6 molecules/particle. They are expected to have a proton affinity close to 220 kcal/mol, similar to that of $CH_3(CH_2)_6NH_2$.[23] Therefore, as the acidified particles are introduced into the ion trap in a positively charged spray, their surfaces should be predominantly covered with protons rather than other competing cations, such as Na^+. Figure 2 displays an anticipated structure of such proton-covered amino-polystyrene microspheres produced by the ESI. Some of the amino groups may be easily protonated, but others are not, depending on the nature of the surface structure.

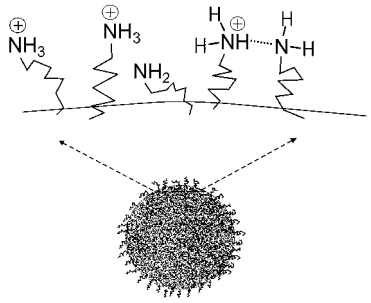

Figure 2. Expected structure of a single protonated amino-polystyrene particle emanated from an electrospray ionization source.

In testing the performance of the ESI, we found that the optimal conditions for generation, trapping, and subsequent analysis of the protonated amino particles involve the use of a concentration of 0.05% (w/v) in 4:1 CH_3OH/H_2O at pH = 3.9. Varying the concentration and acidity over 1 order of magnitude can substantially deteriorate the ESI performance. It should be noted that the concentrations (ranging from 0.005% to 0.5%) used in this experiment are all sufficiently low that there exists at most one single polystyrene microsphere in each nascent spray droplet,[24,25] and agglomeration of the particles in solution is minimal.

Calibration of the SPMS. One limitation in the mass and charge determination of particles in the domain $m/z > 10^6$ is the lack of a proper calibrant for the AF ion trap mass spectrometer, the performance of which may not exactly follow what the Mathieu's equations[9] have predicted because of the existence of the gravitational force, buffer gas, and imperfections (both electronic and mechanical) of the ion trap. Hence, the point of ejection on the stability diagram (a_z vs q_z) may significantly deviate from $q_{eject} = 0.908$ (at $a_z = 0$) in the case of a nonideal ion trap. To calibrate such single-particle mass spectra, we determine the secular frequencies of the oscillatory motions of a single particle within the trap using the method developed by Schlemmer et al.,[16] followed by recording the action of particle ejection in real time to deduce the correlation between the measured secular frequencies and the AF voltage amplitudes at the moment of the ejection.

In this experiment, a beam from a 10 mW He−Ne laser is introduced into the trap through the hole on the lower end cap from the bottom of the chamber. Scattered laser light from the levitated particle is collected by a telescope through the hole on the ring electrode perpendicular to the incident laser beam (cf. Figure 1). Figure 3a displays a video image of the trajectory of the oscillatory motion of a single diamond microparticle (roughly 0.7 μm in diameter) confined within the trap, recorded by using

(21) Schreiner, J.; Voigt, C.; Mauersberger, K.; McMurry, P.; Ziemann, P. *Aerosol Sci. Technol.* **1998**, *29*, 50−56.
(22) Bohren, C. F.; Huffman, D. R. *Absorption and Scattering of Light by Small Particles*; Wiley: New York, 1983.
(23) Hunter, E. P. L.; Lias, S. G. *J. Phys. Chem. Ref. Data* **1998**, *27*, 413−656.
(24) Kebarle, P.; Tang, L. *Anal. Chem.* **1993**, *65*, 972A−986A.
(25) Gomez, A.; Tang, K. *Phys. Fluid* **1994**, *6*, 2317−2332.

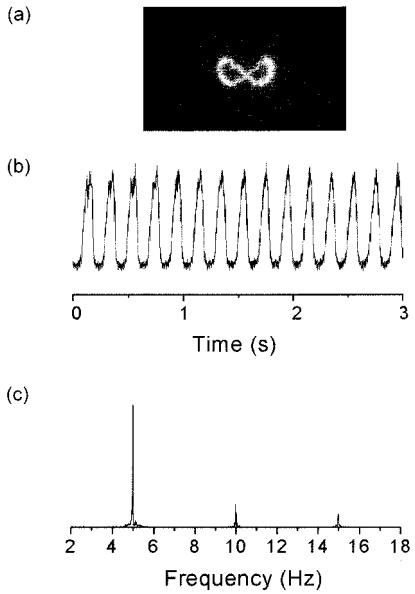

Figure 3. (a) Video image of the trajectory of the oscillatory motion of a single charged microparticle in the quadrupole ion trap recorded by using a CCD camera. (b) Time-domain measurements of the scattered light intensity using a photomultiplier tube. Modulation of the signal was made with use of a vertical slit to block out one-half of the scattered laser light to reveal the radial secular frequency, ω_r. (c) Fourier transform of the time-domain spectrum shown in b. The fundamental frequency of the secular motion is determined to be $\omega_r/2\pi = 4.990 \pm 0.007$ Hz, and its harmonics can also be detected at $2\omega_r$ and $3\omega_r$ in the same spectrum.

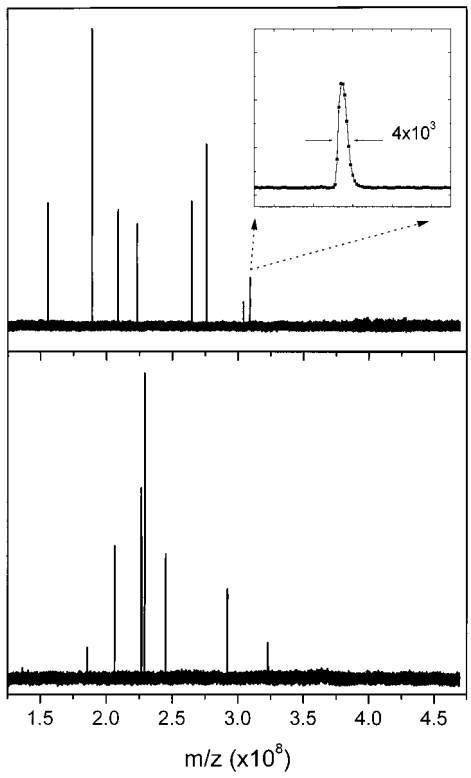

Figure 4. Single-particle mass spectra observed in two independent ESI and trapping events. The spectra were taken for the same amino-polystyrene suspension at pH = 3.9, showing a nearly random distribution of the mass-to-charge ratios of the dispersed particles. The individual peak observed in the spectrum is essentially derived from one single particle. Inset: Enlarged view of a typical scattered laser light pulse from a single polystyrene particle ejected out of the ion trap. The pulse has a fwhm of $\Delta(m/z) = 4 \times 10^3$, suggesting a mass resolution of $m/\Delta m \approx 10^4$ for this single-particle mass spectrometer.

a CCD (charge coupled device) camera. With the aid of a small dc voltage (typically 10 V) applied across the top and bottom end caps to compensate the particle's gravitational force, a near 2:1 Lissajous-type trajectory can be obtained (Figure 3a).[10] The particle oscillates nearly symmetrically above and below the central plane of the ion trap.

To assess the m/z value of this single trapped nanoparticle, the secular frequency of its motion in the radial direction (ω_r) is determined under the condition, $q_z < 0.4$. This is made by collecting the scattered light from the He−Ne laser using a photomultiplier tube. Modulation of the signals (Figure 3b) is established by the use of a set of knife edges to block out one-half of the scattered laser light, that is, the light from either the right half or the left half of the image (Figure 3a). Fourier transform of the time-domain spectrum yields the radial secular frequency (Figure 3c), from which the mass-to-charge ratio is calculated with the formula, $m/z = V_{ac}/\sqrt{2}r_0^2\Omega\omega_r$.[9,26]

RESULTS AND DISCUSSIONS

Single-Particle Mass Spectra. Figure 4 depicts the typical single-particle mass spectra obtained from ESI of a colloidal suspension of amino-polystyrene microspheres at pH = 3.9 and $\Omega/2\pi = 600$ Hz. By using the ESI source as a particle generator, isolation of the spheres in the gas phase is warranted. Shown in Figure 4 are the spectra acquired in two independent experiments using the same suspension. The two spectra look entirely different, with peaks nearly randomly distributed. This feature, together with the Gaussian-like distribution of the peak intensities, strongly suggests that the individual peak in the observed mass spectrum is derived from one single particle. The suggestion is, indeed, confirmed from a direct observation of the action of particle ejection both inside and outside the ion trap using the CCD and the PMT simultaneously. One may attribute the differences in peak height between different particles in the same spectrum to the Gaussian profile of the laser beam, because not all of the ejected particles traverse through the beam at the same spot and, hence, experience the same illumination intensity. Such a site effect has similarly been observed in single-molecule detection of fluorescent chromophores either immobilized in a solid matrix[27] or flowing in a water stream.[28]

An analysis of the time profile of each peak in the spectrum reveals the velocity of the particle leaving the trap. The inset in Figure 4 exhibits an enlarged portion of a high-resolution spectrum encoded by 3.0×10^5 data points acquired in 12 s. A typical time profile with a full width at the half-maximum (fwhm) of 200 μs is recorded. This fwhm corresponds to an ion velocity of 15 m/s for a particle traversing through the laser beam with a diameter of 3 mm (at the $1/e^2$ intensity points). Notably, the velocity is about 1 order of magnitude lower than the corresponding velocity

(26) Cai, Y.; Peng, W.-P.; Kuo, S.-J.; Chang, H.-C. *Int. J. Mass Spectrom.*, in press.

(27) Moerner, W. E. *Sci.* **1994**, *265*, 46−53.

(28) Nguyen, D. C.; Keller, R. A.; Jett, J. H.; Martin, J. C. *Anal. Chem.* **1987**, *59*, 2158−2161.

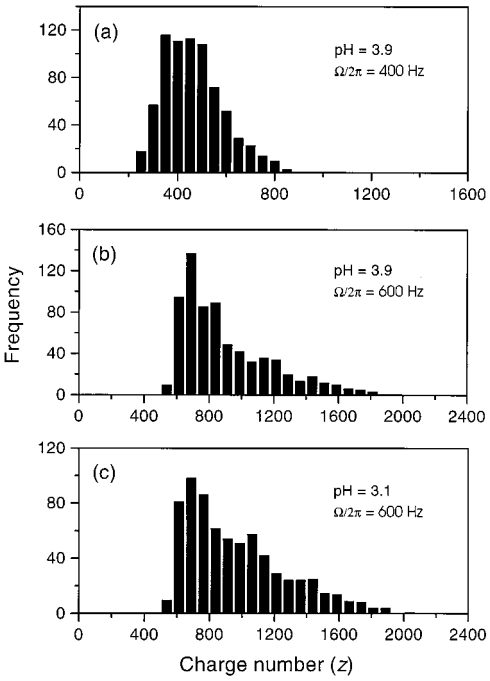

Figure 5. Dependence of the charge-state distribution on trapping frequency and acidity of the spray solutions under different experimental conditions. The histogram of the respective charge-state distribution is deduced on the basis that the particle has a mean diameter of 0.91 μm and a density of 1.05 g/cm^3.

(320 m/s) of the particles in an aerosol beam,[7] presumably because of the lack of an inflow of gas through the ion trap in the present experiment.

A proper interpretation of the single-particle mass spectra relies on explicit statistical analysis. We accomplished the analysis after a collection of roughly 700 particles from 100 repetitions of the experiment using the same polystyrene colloidal suspension [0.02% (w/v), pH = 3.9], from which a histogram of the charge state distribution is obtained. Figure 5a displays a typical distribution for particles trapped at $\Omega/2\pi = 400$ Hz. It is a log-normal[29] type of distribution, and an average charge state of $z = 460$ protons is determined for particles having a mean mass of $m = 4.1 \times 10^{-16}$ kg. The uncertainty in this charge state determination is $\pm$ 30, a result of the mass dispersion (7%).

The presently observed charge state distribution depends not only on the particle concentration and solution acidity, but also on trapping conditions. Such an effect manifests itself when the output frequency of the AF power supply is varied. The distributions shown in Figure 5a,b reveal a shift of the charge states to higher values as the AF is increased from 400 to 600 Hz for the same particles in the same suspension. One can fully understand this frequency dependence in terms of the solutions to the Mathieu equations that an increase in the trapping frequency would promote the trap to confine particles having a larger charge-to-mass ratio.[9]

The capability of single particle detection in this experiment is noteworthy. It affords a mass resolution of $m/\Delta m \approx 10^4$ in the absence of ion ensemble effects. March and co-workers[30,31] recently delineated in detail the effect as well as the circumstances of how improvement in mass resolution can be achieved with the quadrupole ion trap mass spectrometer. The improvement includes axial modulation and scanning the ac voltage amplitude at a slower rate. As described by the authors,[31] the basic principle behind the axial modulation to establish high resolution is that the modulation enlarges the ion cloud such that the range of effective working points of an ion ensemble being ejected out of the ion trap is reduced. This subsequently reduces the width of the associated peaks in the observed spectrum. A similar rationale on the ion ensemble effect has also been given by Cooks and co-workers.[32]

The present SPMS opens new opportunities for performing high-resolution mass spectrometry for nanometer-sized and micrometer-sized particles. The method is free of ion ensemble effects, and hence, achieving a mass resolution ($m/\Delta m$) of the order of 10^6 is feasible. One can realize this high-resolution mass spectrometry via implementation of the proven techniques, such as (1) increasing the precision for the AF voltage amplitude control,[20] (2) scanning the AF voltage amplitude at a slower rate,[20] (3) phase locking and line locking of the AF power source,[33] and (4) reducing both the axial and radial distributions[34] of the particles with caution. Before the implementation of these techniques is realized, the accuracy of the m/z measurement is limited to about 10^{-3}, as the present experiment has established.[26]

Surface Charge States. The number of charges presently obtained for the polystyrene microspheres lies within the range 10^2–10^3. Lowering the pH values of the suspensions does not seem to increase significantly the number of charges on these amino-polystyrene particle surfaces. Figure 5b,c compares the charge-state distribution observed for the suspensions of pH = 3.9 and 3.1, respectively, revealing a weak pH dependence. The average number of the charges increases from 900 to 960 as the pH value of the suspension decreases from 3.9 to 3.1. This weak pH dependence is in line with the conclusion reached by Carbeck et al.[35] about biopolymers that distribution of the charge states of proteins produced in the gas phase by ESI is not directly correlated with the net charges of the corresponding proteins in solution.[36,37]

The average charge number of about 10^3/particle is far below that predicted by the Coulomb repulsion model, which suggests that a liquid droplet of 1 μm in diameter can accommodate up to 10^6 charges on its surface before the Rayleigh stability limit is reached.[24,25] Such a number (10^3/particle) is also about 3 orders of magnitude lower than that of the aminoheptyl groups on the polystyrene particle surfaces, that is, 3×10^6 groups/particle. In the search for the maximum number of charges, we used a higher trapping frequency, a lower AF voltage amplitude,

(29) Hunter, R. J. *Foundations of Colloid Science*; Clarendon Press: Oxford, 1986; Vol. I.
(30) March, R. E. *Int. J. Mass Spectrom.* **2000**, *200*, 285–312.
(31) Londry, F. A.; Wells, G. J.; March, R. E. *Rapid Commun. Mass Spectrom.* **1993**, *7*, 43–45.
(32) Cox, K. A.; Cleven, C. D.; Cooks, R. G. *Int. J. Mass Spectrom. Ion Processes* **1995**, *144*, 47–65. Cleven, C. D.; Cox, K. A.; Cooks, R. G.; Bier, M. E. *Rapid Commun. Mass Spectrom.* **1994**, *8*, 451–454.
(33) Londry, F. A.; March, R. E. *Int. J. Mass Spectrom. Ion Processes* **1995**, *144*, 87–103.
(34) Cleven, C. D.; Cooks, R. G.; Garrett, A. W.; Nogar, N. S.; Hemberger, P. H. *J. Phys. Chem.* **1996**, *100*, 40–46.
(35) Carbeck, J. D.; Severs, J. C.; Gao, J.; Wu, Q.; Smith, R. D.; Whitesides, G. M. *J. Phys. Chem. B* **1998**, *102*, 10596–10601.
(36) Wang, G.; Cole, R. B. *Org. Mass Spectrom.* **1994**, *29*, 419–427.
(37) Zhou, S.; Cook, K. D. *J. Am. Soc. Mass Spectrom.* **2000**, *11*, 961–966.

and more acidic solutions for the ESI, but found that the probability of having a trapped particle containing more than 10^4 charges is low.[38] Whereas one might expect the maximum number of the charges that a particle can accommodate should be equal or close to the number of the surface functional groups, this is apparently not the case in the present observations.

The observation of a lower charge state than expected may be rationalized as follows: First, the sample contains rigid solid spheres, the shape of which does not vary with the number of charges held. Hence, the charge state would depend mainly on how the amino groups are distributed on the particle surfaces. It is likely that the distribution of these surface amino groups is not uniform and the charge repulsion is not so fully minimized as described by the model.[25] Some of the groups may cluster together, forming relatively strong ionic hydrogen bonding[39] between adjacent units (Figure 3) and preventing complete protonation of the surface from occurring. Second, the charging mechanism during the ESI is governed by protonation, and conversely, discharging is promoted by deprotonation. Thus, the number of surface protons, once produced, may be reduced successively via ion−molecule reactions or charge uptake from the walls along the way in the beam tubes (Figure 1) before the particles reach the trap entrance. Such deprotonation reactions can further take place via collision-induced proton transfer with background gas molecules, presumably H_2O, within the trapping device.[40]

Applications. The SPMS is applicable to investigation of particles of smaller sizes as well. We have successfully employed this technique to detect diamond nanocrystals of a nominal diameter of 100 nm. To obtain the spectrum of these particles, the sample (Kay Industrial Diamond SJK-5) was first oxidized in air at 600 °C for 1 h to ensure that their surfaces were covered with ether, carbonyl, or carboxylic groups.[41] With these functional groups on the surfaces, the particles were ready to accept protons from acetic acid during the ESI. A 4:1 CH_3OH/H_2O mixture containing 0.02% (w/v) of the particles at pH = 3.9 was used as the spray solution in this experiment.

Given in Figure 6 is the mass spectrum of diamond nanocrystals, which are all irregular in shape and differ markedly in size. Some of them have rough surfaces, and others are in the form of aggregates composed of smaller particles of ~40 nm in diameter. Noteworthy, however, is that although the particles are all nearly 10-fold smaller than the corresponding polystyrene microspheres discussed earlier, spectra with a signal-to-noise ratio exceeding 20 can readily be obtained. The achievement is conceivably due to the unusual properties of diamond, which has an exceptionally large refractive index of $n \approx 2.4$ in the visible region.[42] Assigning an estimated mass of 1.5×10^{-17} kg to each particle, the average

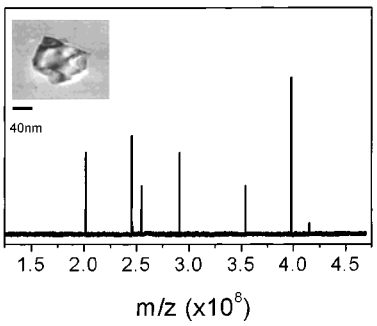

Figure 6. Single-particle mass spectrum of diamond nanocrystals. Inset: Photograph of a typical diamond nanocrystal, taken by using a transmission electron microscope. The nominal diameter of the particles is 100 nm.

number of the excess protons on these nanodiamonds is roughly 50/particle.

The present observation suggests an interesting application of the SPMS to the identification of both micrometer-sized and nanometer-sized bioparticles, such as bacteria spores[43] and bacteriophages,[6] in the gas phase. The coliphages T4, T5, and T7,[44] each having a molecular weight of the order of 10^8 Da, clearly serve as good examples. In investigating these particles, one may suffer the difficulty that they have low refractive indexes, close to that of liquid water. According to the Rayleigh-Debye theory,[22] the intensity of scattered light depends sensitively on the particle radius, refractive index, and incident laser wavelength as $I \propto a^6(n^2 - 1)^2/\lambda^4(n^2 + 2)^2$, which is valid for a homogeneous sphere with $a(n - 1)/\lambda \ll 1$ in a vacuum. The theory predicts a reduction of the signal by a factor of 10 if the same experiment described above for nanodiamonds is performed for bioparticles of $2a = 100$ nm and $n = 1.3$. Fortunately, this reduction can be easily compensated by using lasers with shorter wavelengths (such as the frequency-doubled Ar-ion laser) as the excitation light source. It suggests that mass analysis of single bioparticles of 100 nm in diameter is practical with this SPMS.

CONCLUSION AND FUTURE WORK

We have developed a novel mass spectrometric method, the single-particle mass spectrometry (SPMS), to interrogate the mass and charge states of submicrometer-sized particles with a $m/z > 10^6$. It is a new form of mass spectrometry, free of ion ensemble effects, and can be regarded as a complementary method to the ESI−FTICR spectrometry in terms of the mass range it covers. Benefiting from single-particle detection, the method is capable of providing a mass resolution ($m/\Delta m$) as high as 10^4. We have successfully demonstrated the capability of this approach using polystyrene microspheres and diamond nanocrystals as examples.

It is desirable to apply the SPMS to determine simultaneously both the absolute mass and charge state of single bioparticles. This conceivably can be accomplished by employing an image-current detection tube[5,6,45] to measure the absolute charge

(38) In a closely related experiment, Fuerstenau and Benner (ref 5) reported observations of 2500 positive charges on 314 ± 16-nm polystyrene particle surfaces. However, these particles are not surface-modified, and thus, the nature of these charges, which can be H^+, Na^+, or other cations, is not well-characterized.

(39) Meot-Ner, M.; Speller, C. V. *J. Phys. Chem.* **1986**, *90*, 6616−6624.
(40) See, for example: McLuckey, S. A.; Wells, J. M.; Stephenson, J. L., Jr. *Int. J. Mass Spectrom.* **2000**, *200*, 137−161.
(41) Ando, T.; Yamamoto, K.; Ishii, M.; Kamo, M.; Sato, Y. *J. Chem. Soc. Faraday Trans.* **1993**, *89*, 3635−3640.
(42) Edwards, D. F.; Philipp, H. R. In *Handbook of Optical Constants of Solids*; Polik, E. D., Ed.; Academic Press: New York, 1985.
(43) Sinha, M. P.; Platz, R. M.; Vilker, V. L.; Friedlander, S. K. *Int. J. Mass Spectrom. Ion Processes* **1984**, *57*, 125−133.
(44) Bancroft, F. C.; Freifelder, D. *J. Mol. Biol.* **1970**, *54*, 537−546. Dubin, S. B.; Benedek, G. B.; Bancroft, F. C.; Freifelder, D. *J. Mol. Biol.* **1970**, *54*, 547−556.
(45) Benner, W. H. *Anal. Chem.* **1997**, *69*, 4162−4168.

numbers of the particles after they pass through the illuminating laser beam. With use of a gated linear ion trap[45] as the detector, the charge state can be determined within $\Delta z = \pm 2$ for particles carrying more than 250 charges. Implementation of this state-of-the-art detector may make the SPMS a useful device in practical applications. The most appealing application of this technique can be found in the human genomic sequencing projects, because the tool appears ideal for the identification of chromosomal fragments with a mass unit on the order of 10^{10} Da. Experiments of these types are now in progress in our laboratories.

ACKNOWLEDGMENT

We are indebted to Profs. D. Gerlich and S. Schlemmer for many fruitful discussions. We also thank the Academia Sinica and the National Science Council (Grant no. NSC 89-2113-M-001-081) of Taiwan for financial support of this work.

Received for review July 10, 2001. Accepted October 11, 2001.

AC010776Y